Pricing rainfall derivatives in the equatorial Pacific

Sergio Cabrales, Jesus Solano and Carlos Valencia
Department of Industrial Engineering, Universidad de los Andes, Bogotá, Colombia, and
Rafael Bautista
School of Management, Universidad de los Andes, Bogotá, Colombia

Received 26 September 2019
Revised 17 January 2020
20 March 2020
Accepted 22 March 2020

Abstract

Purpose – In the equatorial Pacific, rainfall is affected by global climate phenomena, such as El Niño Southern Oscillation (ENSO). However, current publicly available methodologies for valuing weather derivatives do not account for the influence of ENSO. The purpose of this paper is to develop a complete framework suitable for valuing rainfall derivatives in the equatorial Pacific.

Design/methodology/approach – In this paper, we implement a Markov chain for the occurrence of rain and a gamma model for the conditional quantities using vector generalized linear models (VGLM). The ENSO forecast probabilities reported by the International Research Institute for Climate and Society (IRI) are included as independent variables using different alternatives. We then employ the Esscher transform to price rainfall derivatives.

Findings – The methodology is applied and calibrated using the historical rainfall data collected at the El Dorado airport weather station in Bogotá. All the estimated coefficients turn out to be significant. The results prove more accurate than those of Markovian gamma models based on purely statistical descriptions of the daily rainfall probabilities.

Originality/value – This procedure introduces the novelty of incorporating variables related to the climatic phenomena, which are the forecast probabilities regularly published for the occurrence of El Niño and La Niña.

Keywords Weather derivatives, Rainfall, ENSO, Esscher transform

Paper type Research paper

1. Introduction

Weather derivatives are financial instruments that hedge the risk associated with unexpected or adverse weather conditions (Jewson and Brix, 2005; Alexandridis and Zapranis, 2013). Their payoffs depend on the values of underlying weather variables, such as rainfall, temperature, wind, solar irradiance, snowfall and humidity (Cao and Wei, 2004). Organizations and individuals have used weather derivatives as part of risk management strategies to cover non-catastrophic weather events (Alexandridis and Zapranis, 2013). The Chicago Mercantile Exchange (CME) estimated that nearly 30% of the US economy and 70% of US companies are exposed to weather risk (CME, 2005). However, pricing these financial instruments is difficult, because the data collection accuracy can be affected by extreme weather or systematic errors; besides, the historical record is short and the statistical properties can be complex (Xu *et al.*, 2008; Dischel, 2000; Little *et al.*, 2009; Cabrera *et al.*, 2013).

According to the Weather Risk Management Association (WRMA), approximately 53% of the over-the-counter (OTC) weather derivatives transactions are based on temperature, and 23% are based on rainfall (WRMA, 2011). The considerable gap between the uses of temperature and rainfall derivatives makes it difficult to estimate the value of the underlying asset (Cabrera *et al.*, 2013). In contrast to the daily average temperature and daily wind speed, the daily rainfall is a binary event that cannot be modeled using geometric Brownian motion (GBM) or a mean-reverting (MR) stochastic process using seasonality for the mean and variance (Wilks, 2011; Benth and Benth, 2013; Alexandridis and Zapranis, 2013).

Agricultural Finance Review
Vol. 80 No. 4, 2020
pp. 589-608

0002-1466
DOI 10.1108/AFR-09-2019-0105

Agriculture is the sector that depends most on precipitation patterns, and the weather is one of the most uncontrollable and unpredictable factors (Alexandridis and Zapranis, 2013). Several risk management strategies have emerged in the agricultural sector because these producers need either precipitation derivatives or insurance (Turvey, 2001; Martin *et al.*, 2001). Unlike insurance contracts, which cover low-probability and high-risk events, such as extreme temperatures, hurricanes or floods, weather derivatives usually shield revenues against high-probability and low-risk events (Cabrera *et al.*, 2013). Moreover, developers and users of hydroelectric power generators and the retail, travel, transportation and construction industries, as well as the government, are also interested in using precipitation derivatives since, in the coming years, gradual increases in both rainfall and temperature variations due to global climate change are expected (Grimm and Tedeschi, 2009).

There are two main fields of study in the literature on rainfall derivatives. The first deals with accurately modeling the frequency and intensity of precipitation over time. The most common and successful approach to simulating rainfall is the Markov chain extended with rainfall prediction (MCPR), which was developed by Wilks (1998). The MCPR has two stages; the first produces a sequence of wet and dry days using a Markov chain, and the second generates a random rainfall amount for each wet day in the sequence. Recently, Leobacher and Ngare (2011) extended the MCPR to a Markovian gamma model that incorporates seasonality into the rainfall process. First-order Markov models are also used in other weather prediction applications (Cao *et al.*, 2004; Odening *et al.*, 2007; Goncu, 2011).

The second field of study deals with pricing rainfall derivatives. Rainfall options can be priced using a burn analysis (Cao *et al.*, 2004; Jewson and Brix, 2005; Spicka and Hnilica, 2013), a utility indifference (Carmona and Diko, 2005; Brockett *et al.*, 2006; Xu *et al.*, 2008; Lee and Oren, 2010; Härdle and Osipenko, 2011; Leobacher and Ngare, 2011), or an Esscher transform (Cabrera *et al.*, 2013). The burn analysis has difficulties predicting the occurrence of extreme precipitation events, and the utility indifference approach is too sensitive to utility function and its parameters (Carr *et al.*, 2001; Jewson and Brix, 2005). Therefore, we elaborate only Esscher transform because it preserves the structure of some traditional stochastic processes and the independent increment property (Cabrera *et al.*, 2013).

It is well established that the El Niño Southern Oscillation (ENSO) has a significant impact on monthly and seasonal rainfall extremes in the equatorial Pacific (Grimm and Tedeschi, 2009; Ropelewski and Halpert, 1987; Aceituno, 1988). Changes caused by the shift disrupt large-scale air movements in the tropics, triggering a cascade of global side effects, as shown in Figure 1. Tropical Pacific warming (El Niño) and cooling (La Niña) events are identified by subsurface ocean temperature indices, including the Oceanic Niño Index (ONI), the Southern Oscillation Index (SOI), the Trans-Niño Index (TNI), the Multivariate ENSO Index (MEI), the Pacific Decadal Oscillation (PDO), Niño1, Niño2, Niño1+2, Niño3, Niño4, Niño3.4 and the Trans-Niño Index (TNI) (Yu *et al.*, 2011; NOAA, 2018). The National Oceanic and Atmospheric Administration (NOAA), using a threshold of $\pm 0.5^{o}$C for the ONI, identifies the onset of El Niño (warm) and La Niña (cold) episodes. However, the ONI is only a set of historical data, and there is no forecast model associated with it. This constitutes an obstacle on the way to pricing rainfall derivatives for the equatorial Pacific. We posit that integrating the effects of the ENSO should improve rainfall prediction models, and therefore, the pricing of rainfall derivatives for this specific area. In this study, we develop a risk-neutral Markovian gamma model built from the monthly seasonality and the ENSO forecast probabilities computed monthly by the International Research Institute for Climate and Society (IRI) using vector generalized linear models (VGLMs).

In section 2, we review the mathematical formulation of the daily rainfall model, as well as the general framework for pricing weather derivatives. Section 3 describes the area under

Note(s): El Niño is the warm phase of a recurring climate pattern across the equatorial Pacific, based on data provided by NOAA (2019) of sea surface temperature anomaly during a strong El Niño (1997)

(a)

Note(s): La Niña is the cool phase of a recurring climate pattern across the equatorial Pacific, based on data provided by NOAA (2019) of sea surface temperature anomaly during a strong La Niña (1988)

(b)

Figure 1.
Sea surface temperature anomaly during El Niño and La Niña

study and some Monte Carlo simulation results for pricing simple European options. Finally, in Section 4, we present summaries of the findings and concluding remarks.

2. Methodology

2.1 Precipitation model

Precipitation can be forecasted using either meteorological or statistical models. The meteorological models are limited by the short-term forecasting horizon and the technical complexity of the implementation (Cabrera *et al.*, 2013). On the other hand, statistical models use data-driven techniques to fit the daily or monthly rainfall data to some well-known probability distribution (Coles *et al.*, 2003). Daily models can be used in order to derive any rainfall index on a daily, monthly or yearly basis.

To develop a better framework for forecasting precipitation in the equatorial Pacific, we follow the baseline approach presented in Wilks (1998, 2011) and Alexandridis and Zapranis (2013). They model the rainfall process using a first-order, two-state Markov process, that is, the probability of the rain event only depends on the previous observation. The daily amount is modeled by a gamma distribution.

The present formulation is an extension of Wilks (1998) that integrates the effects of ENSO and the monthly effects into models of the rainfall amount and frequency. Pricing the rainfall derivatives then follows a risk-neutral approach by employing the Esscher transform as formalized in Gerber and Shiu (1994, 1996) and Cabrera *et al.* (2013). With this approach, we use daily data and take advantage of the availability of meteorological observations on this time scale.

In modeling the rainfall process, we follow the baseline approach described in Wilks (1998), which consists of two stages. The first stage models the frequency of precipitation, and the second models the amount. We propose four models to include the effects of El Niño and La Niña in the rainfall derivative prices where Model 1 is not a two-stage model, but we use it as a benchmark:

(1) Model 1: The monthly rainfall amount (rainfall index) is modeled by a gamma distribution with equal parameters (μ and shape) for every month.

(2) Model 2: The monthly rainfall amount is modeled separately using a precipitation frequency process and a precipitation amount process. We assume that the rainfall frequency is a two-state Markov process, the daily rainfall amount is a gamma process, and both processes are conditionally independent given the month.

(3) Model 3: The monthly rainfall amount is modeled independently. We assume that the daily rainfall frequency is a two-state Markov process, the daily rainfall amount is a gamma process, and both processes are affected by the month and the forecast probability of El Niño ($p^{\text{Niño}}$).

(4) Model 4: The monthly rainfall amount is modeled independently. We assume that the rainfall frequency is a two-state Markov process, the daily rainfall amount is a gamma process, and both processes are affected by the month and the difference between the forecast probabilities of El Niño and La Niña ($p^{\text{Niño}} - p^{\text{Niña}}$).

2.1.1 Precipitation frequency process. The occurrence of daily precipitation is commonly modeled as a Markov process (Moreno, 2002; Cao *et al.*, 2004; Odening *et al.*, 2007; Goncu, 2011). The daily rainfall amount R_i on day i is the product of a random rainfall amount r_t and a rainfall occurrence process X_i:

$$R_i = r_i X_i \tag{1}$$

The amount process and the occurrence process are modeled separately and are independent. Days are defined as wet if the amount of precipitation is greater than the minimum of 0.01 inches; otherwise, they are dry. X_i represents whether precipitation occurred on day i:

$$X_i = \begin{cases} 0 & \text{if day } i \text{ is dry,} \\ 1 & \text{if day } i \text{ is wet.} \end{cases} \tag{2}$$

Since X_i is modeled as a first-order Markov chain, the precipitation state for any day is fully determined by the precipitation state on the previous day. Thus, the day-to-day transition probabilities for reaching a given state on day i given the state at $i-1$ are:

$$p_i^{00} = Pr(X_i = 0 | X_{i-1} = 0), \tag{3a}$$

$$p_i^{01} = Pr(X_i = 1 | X_{i-1} = 0), \tag{3b}$$

$$p_i^{10} = Pr(X_i = 0 | X_{i-1} = 1), \tag{3c}$$

$$p_i^{11} = Pr(X_i = 1 | X_{i-1} = 1). \tag{3d}$$

The conditional probabilities p_i^{01} and p_i^{11} are sufficient to specify their respective Markov processes because the components of the probability vectors must separately add to 1.

In the literature, transition probabilities are usually estimated using maximum likelihood estimation (MLE) (Wilks, 1998; Cao *et al.*, 2004; Alexandridis and Zapranis, 2013):

$$\widehat{p}_i^{01} = \frac{n_j^{01}}{n_j^{00} + n_j^{01}} \tag{4}$$

$$\widehat{p}_i^{11} = \frac{n_j^{11}}{n_j^{10} + n_j^{11}} \tag{5}$$

where n_j^{01} and n_j^{11} are the historical counts for month j of transitions from dry days to wet days and wet days that follow wet days, respectively. The quantities n_j^{01} and n_j^{11} have the equivalent interpretation for wet days. However, these transition probabilities do not take proper account of ENSO. The lack of a clear deterministic trend in the occurrence of the different states of the ENSO phenomenon dilutes its true impact when the estimated daily rainfall probabilities come from simple MLE. In other words, the estimation of the probabilities of transition from dry/wet days to wet days is performed without considering the presence of El Niño or La Niña. Further elaborations, such as the use of truncated Fourier approximations (Cabrera *et al.*, 2013), still make strong assumptions about some kind of underlying regular seasonality. In this paper, instead of pursuing purely statistical means, we choose to include variables that foretell the actual ENSO-related phenomena.

In order to include the effects of the ENSO, we propose the use of vector generalized linear models (VGLMs) to estimate the necessary parameters from which to describe the daily rainfall probabilities. The response variable is the day-ahead precipitation state X_i given a current state X_{i-1}. Since X_i follows a Bernoulli distribution, its expected value is $p_i^{X_{i-1}1}$.

The focus is then on specifying a VGLM that connects these probabilities with explanatory factors that relate them to physical conditions that may foretell the states of ENSO. One is the calendar month, which is represented by a categorical variable with an index that runs from 1 to 12. The others are the probability forecasts for the ENSO categories issued every month by the International Research Institute for Climate and Society (IRI). Among the IRI conventions is one that separates the states into three ENSO categories: El Niño, La Niña and neutral. The forecast probabilities for these categories should add to 1. The data used for the ensuing analysis come from the IRI website. These forecast probabilities are the result of averaging twenty forecasts produced by various institutions. Over the last few decades, those institutions have developed different approaches to ENSO state assessment and short-term prediction whose characters range from statistical to dynamical (Barnston *et al.*, 2012).

Our proposed models (Model 2, Model 3 and Model 4) use the logit function as the link function. Thus, our generalized linear model for each initial state is:

Initial state: $X_{i-1} = 0$

$$\ln\left(\frac{p_i^{01}}{1-p_i^{01}}\right) = \beta_{01}^{2T} M \tag{6a}$$

$$\ln\left(\frac{p_i^{01}}{1-p_i^{01}}\right) = \beta_{01}^{3T} M + \beta_{02}^{3} p_j^{\text{Niño}} \tag{6b}$$

$$\ln\left(\frac{p_i^{01}}{1-p_i^{01}}\right) = \beta_{01}^{4T} M + \beta_{02}^{4}\left(p_j^{\text{Niño}} - p_j^{\text{Niña}}\right) \tag{6c}$$

Initial state: $X_{i-1} = 1$

$$\ln\left(\frac{p_i^{11}}{1-p_i^{11}}\right) = \beta_{11}^{2T} M \tag{6d}$$

$$\ln\left(\frac{p_i^{11}}{1-p_i^{11}}\right) = \beta_{11}^{3T} M + \beta_{12}^{3} p_j^{\text{Niño}} \tag{6e}$$

$$\ln\left(\frac{p_i^{11}}{1-p_i^{11}}\right) = \beta_{11}^{4T} M + \beta_{12}^{4}\left(p_j^{\text{Niño}} - p_j^{\text{Niña}}\right) \tag{6f}$$

where M is a vector of twelve binary variables that represent the months of the year, with one for each categorical month j. The parameters β_{01}^{h} and β_{11}^{h}, for $h = 2, 3, 4$, are twelve-dimensional vectors that contain the intercepts for each month in every model and β_{01}^{hT} are the transposes. $p_j^{\text{Niño}}$ is the IRI monthly forecast probability for El Niño, and $p_j^{\text{Niña}}$ is the monthly forecast probability for La Niña. A scatter plot of the data available for these two variables reveals a high linear correlation (−0.56). Their historical running averages, called climatological probabilities, tend to follow each other rather closely, but their spot values for any given month, especially when one of these two categories is surging, may divert widely. For these reasons, we choose the difference in probability forecasts as the second option for the explanatory variable.

2.1.2 Precipitation amount process. In the literature, authors have used different probability distributions to model rainfall amounts; these include mixed exponential (Wilks, 1998; Suhaila and Jemain, 2007; Foufoula-Georgiou and Lettenmaier, 1987) and Weibull (Wilks, 1989) distributions. After fitting different probability densities to our data, we propose modeling the precipitation process by fitting the number of wet days to a gamma

distribution. As stated earlier, r_i is the total rainfall amount simulated for any given wet day i. This amount can be modeled as $r_i \sim \text{Gamma}(\kappa, \theta)$, where κ is the shape parameter, and θ is the scale parameter of the distribution.

Because it is necessary to estimate two different parameters, we propose a vector generalized linear model (VGLM) to estimate them. The idea behind this VGLM is to transform each parameter with logarithmic link functions and express this transformation as a linear combination of the chosen predictors. For the last three of the four proposed models, we have:

$$\ln(\mu_j) = \alpha_1^{2T} M \tag{7a}$$

$$\ln(\mu_j) = \alpha_1^{3T} M + \alpha_2^3 p_j^{\text{Niño}} \tag{7b}$$

$$\ln(\mu_j) = \alpha_1^{4T} M + \alpha_2^4 (p_j^{\text{Niño}} - p_j^{\text{Niña}}) \tag{7c}$$

$$\ln(k_j) = \gamma_1^{2T} M \tag{7d}$$

$$\ln(k_j) = \gamma_1^{3T} M + \gamma_2^3 p_j^{\text{Niño}} \tag{7e}$$

$$\ln(k_j) = \gamma_1^{4T} M + \gamma_2^4 (p_j^{\text{Niño}} - p_j^{\text{Niña}}) \tag{7f}$$

where μ_j ($\mu_j = \kappa_j \theta_j$) is the expected precipitation for wet days during specific month j. To fit the model, we filter the full historical dataset by wet days. With the estimated parameters, we simulate a synthetic daily rainfall, which is a gamma-distributed variable with the parameters μ_j and κ_j adjusted for each month.

For any given day, the simulated amount of rainfall r_i is modeled by a gamma distribution $f(r_i; \kappa_j, \theta_j)$. For month j with m days, the simulated total rainfall is

$$I_j(m) = \sum_{i=1}^{m} r_i X_i \tag{8}$$

This is a random variable and conditional on the number of days in month j. It is the random variable representing the rainfall index for month j. The corresponding number of wet days, for the same realization of X_i, is

$$n = \sum_{i=1}^{m} X_i \tag{9}$$

This equation produces an integer with a discrete probability distribution $g_j(n)$, which complies with

$$\sum_{i=1}^{m} g_j(i) = 1, \forall j \in [1, 2, .., 12] \tag{10}$$

This distribution can be elicited from a numerical simulation. Similarly, the continuous distribution of $I_j(m)$ can be partitioned conditional on m: $I_j(n|m)$, with $I_j(n|0) = 0$. This partition is of interest because it permits some analytical simplification. The addition I_j of n independent, identically gamma-distributed random variables is gamma-distributed according to the composition rule (Prabahu, 1965; Moschopoulos, 1985; Mathai, 1982):

$$f(I_j;\kappa,\theta|n) = \frac{\theta^{-n\kappa} I^{n\kappa-1}\exp\left(\frac{-I_j}{\theta}\right)}{\Gamma(n\kappa)} \tag{11}$$

By using this result, the probability distribution function for I_j can be written as:

$$f(I_j;\kappa,\theta) = \sum_{n=1}^{m} \frac{\theta^{-n\kappa} I_j^{n\kappa-1}\exp\left(\frac{-I_j}{\theta}\right)}{\Gamma(n\kappa)} g_j(n) \tag{12}$$

This is then the probability distribution, computed with the shape and scale parameters estimated for each month j, for the distribution of the monthly-accumulated index I_j.

2.2 Weather derivative pricing

We now turn to the problem of pricing simple, European options using a rainfall index. Rainfall options can be priced using burn analysis. Burn analysis tries to derive an empirical distribution of the rainfall index using historical rainfall data (Cao *et al.*, 2004; Jewson and Brix, 2005; Spicka and Hnilica, 2013). With the empirical distribution, the payoff is determined and discounted with the risk-free rate. Although this method is widely used to price rainfall derivatives, Cao *et al.* (2004) found that derivative prices produced by burn analysis are highly sensitive to historical observations. Additionally, Jewson and Brix (2005) state that burn analysis has difficulties predicting the occurrence of extreme rainfall events, such as those produced by strong ENSO conditions.

There are also attempts that use the utility indifference approach. Carmona and Diko (2005) assume the existence of tradable rainfall assets. Brockett *et al.* (2006) and Xu *et al.* (2008) assume a market with a seller and a buyer and account for the correlation between the weather index and risky assets. Lee and Oren (2010) and Härdle and Osipenko (2011) simulate market conditions between financial investors and farmers to find equilibrium prices, and Leobacher and Ngare (2011), assuming that weather-sensitive security exists, extend the pricing methods to include seasonality. Nevertheless, the utility indifference approach is too sensitive to preferences and to the risk aversion parameter (Carr *et al.*, 2001).

Following a different approach, Cabrera *et al.* (2013) show how the Esscher transform Esscher (1932) is ideally suited to price rainfall futures since it preserves the independent increment property and the structure of some traditional stochastic processes. Classical asset pricing theory starts with the assumption of a complete market. However, the market for weather derivatives is incomplete in the sense that the underlying indices are non-tradable and cannot be perfectly replicated by financial assets (Xu *et al.*, 2008; Cabrera *et al.*, 2013). Gerber and Shiu (1994) showed how, with the assumption that returns follow a normal distribution, it is possible to price derivatives contracted over underlying indexes that do not directly trade in capital markets. For incomplete markets, they approach derivative pricing by constructing a risk-neutral measure using the Esscher transform. To achieve this, they assume there is a single trader who is expected to maximize utility.

The Esscher transform maps a probability density function $f_P(x)$ of a random variable x into a new probability density function $f_Q(x;\pi)$:

$$f_Q(x;\pi) = \frac{\exp(\pi x) f(x)}{\int_{-\infty}^{\infty}\exp(\pi x) f(x)dx} \tag{13}$$

where π is a measure of risk aversion called the market price of risk (MPR). It is used to calibrate the risk-neutral expectation such that observed market prices and risk-neutral

prices match (Cabrera *et al.*, 2013; Noven *et al.*, 2015). After integrating the denominator (Appendix), the Esscher transformation of the index probability function in equation (12) is:

$$f_Q(I_j;\pi,\kappa,\theta)=\frac{\exp(\pi I_j)\sum_{n=1}^{m}\frac{\theta^{-n\kappa}I_j^{n\kappa-1}\exp\left(\frac{-I_j}{\theta}\right)}{\Gamma(n\kappa)}g_j(n)}{\sum_{n=1}^{m}\frac{g(n)}{\left(I_j[\pi\theta-1]\right)^{(n\kappa)}}} \tag{14}$$

The next step in pricing the rainfall option is to use equation (14) as the risk-neutral expectation of payoff associated with the underlying weather index. For a rainfall option sold for month i with the final index value denoted by I_i, the prices of the European call and put options with strike level K are:

$$c_j=e^{-rT}E[\alpha\max(I_j-K,0)] \tag{15}$$

$$p_j=e^{-rT}E[\alpha\max(K-I_j,0)] \tag{16}$$

where T is the time to exercise the option, α is the tick size and r is the risk-free rate. The expected values are then obtained via Monte Carlo simulation. It is necessary to choose representative values for the MPR (π).

3. Empirical analysis

To include the impact of El Niño and La Niña in rainfall derivative prices for the equatorial Pacific, we use the daily rainfall data registered at the El Dorado Airport Weather Station located in Bogota, Colombia. The series of daily rainfall amounts (in inches) in this study runs from January 1972 to December 2015. The rainfall data were provided by the Instituto de Hidrología, Meteorologá y Estudios Ambientales (IDEAM) (2019), and the data for the Oceanic Niño Index (ONI) came from the Climate Prediction Center–NOAA (2019a, b, c).

Figure 2 displays the monthly rainfall amounts at the IDEAM weather station at Bogotá's airport between 1972 and 2015. This box-plot shows local rain seasonality with two dry seasons and two wet seasons.

Figure 3 displays the monthly frequency of wet days and reflects a dip in frequency at year-end. These box-plots, rainfall amounts and wet days do not quite follow the same seasonal pattern, with the main divergence between them occurring during the middle of the year.

Figure 4 displays the monthly average precipitation amounts when El Niño, La Niña or neutral occurred. Under El Niño, the monthly precipitation is lower on average than it is under La Niña, except for the month of April. The difference between them is proportionally widest in January when precipitation during El Niño is less than a quarter of the precipitation during La Niña. Throughout most of the year, the neutral state shows intermediate precipitation values.

Figure 5 shows the monthly average number of wet days filtered by the IRI categories El Niño, La Niña and neutral. Throughout the year, the average number of wet days is lower when El Niño occurs than when La Niña occurs, except for the month of April. For average rainy days, the variations along the year are not as marked as for rainfall. The largest difference in averages occurs in January. Under El Niño, the average number of wet days in January is 5.26 versus 9.77 days when La Niña dominates. It is interesting to notice that although the trend of El Niño with respect to the neutral state is roughly as expected, the monthly differences in frequency are not large, except in January and September. Comparing Figures 4 and 5 shows that, expressed as a percentage, the differences in the effects of El Niño

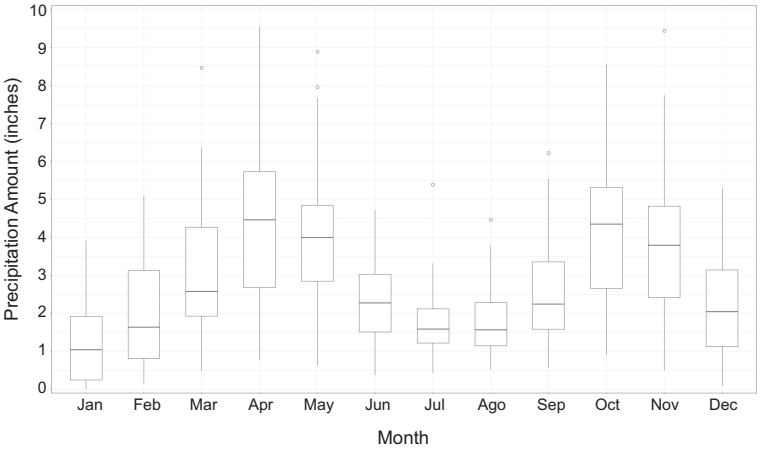

Figure 2.
Monthly rainfall amounts at the El Dorado Airport Station (Bogotá) for 1972–2015

Source(s): Instituto de Hidrología, Meteorologá y Estudios Ambientales (IDEAM) (2019)

and La Niña is more visible through the precipitation amount than through the frequency of wet days.

Unlike previous work, our strategy for constructing a distribution of the monthly rainfall amount (the rainfall index) requires the computation of derivative prices using VGLM estimation to obtain the parameters that characterize the probability density functions in rainfall index simulations. In Cabrera *et al.* (2013), the approach consists of using Fourier analysis to extract parameterizations of the probability density functions from historical data. However, the irregular characteristics of the ENSO phenomenon make this approach

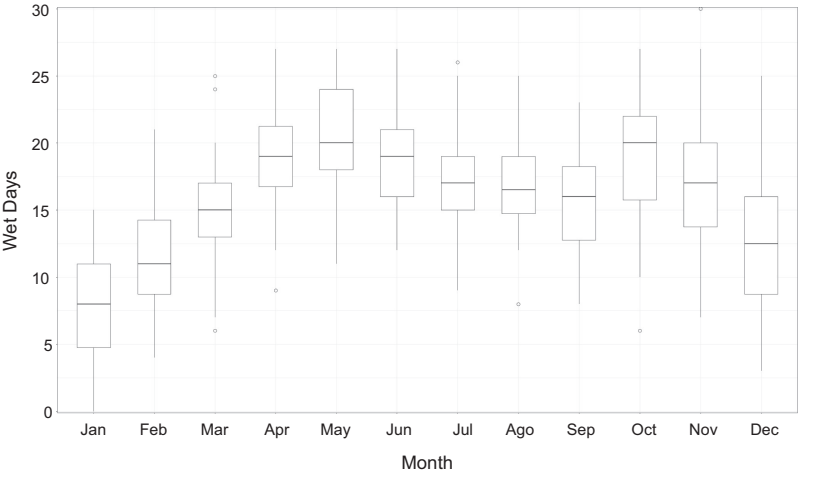

Figure 3.
Monthly frequency of wet days at the El Dorado Airport Station (Bogotá) for 1972–2015

Source(s): Instituto de Hidrología, Meteorologá y Estudios Ambientales (IDEAM) (2019)

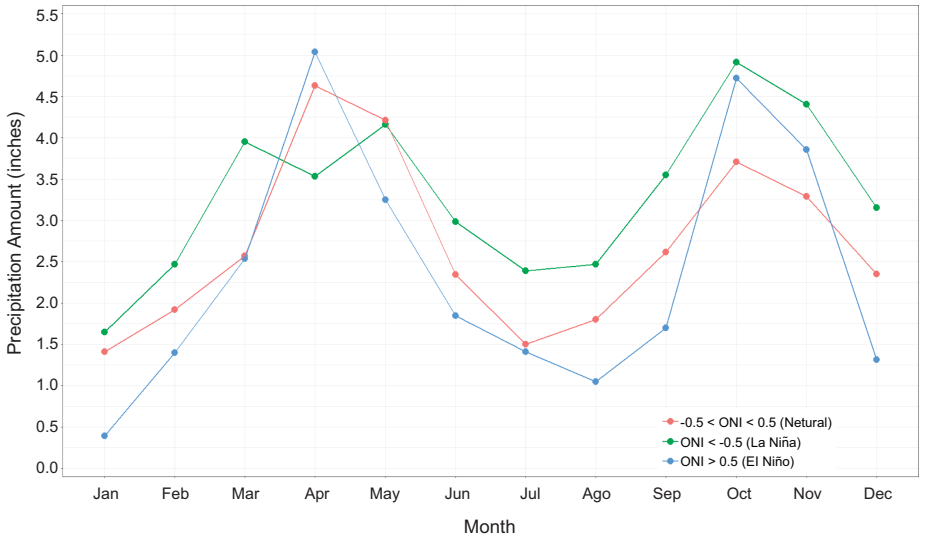

Source(s): Instituto de Hidrologíá, Meteorologá y Estudios Ambientales (IDEAM) (2019)

Figure 4.
Monthly mean precipitation amounts for the El Dorado Airport Station (Bogotá) for 1972–2015 when filtered by the ONI

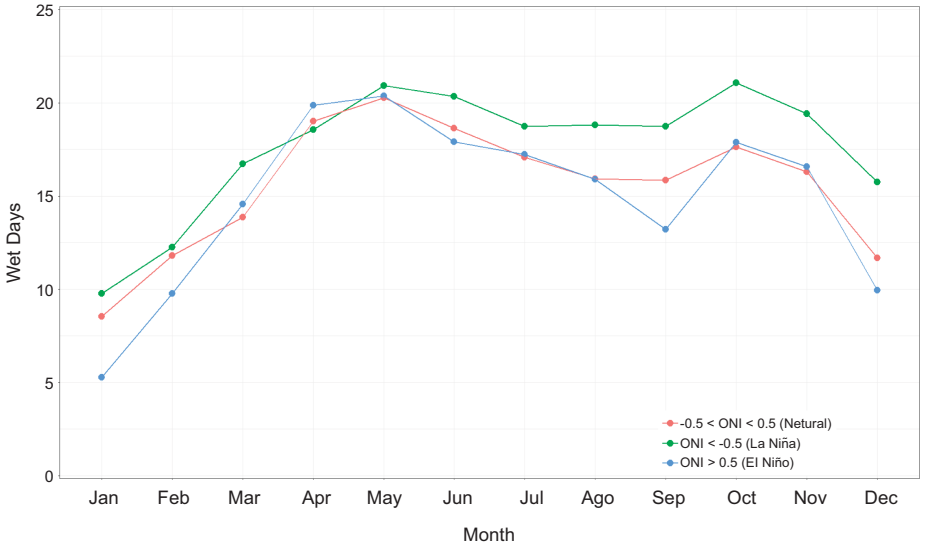

Source(s): Instituto de Hidrologíá, Meteorologá y Estudios Ambientales (IDEAM) (2019)

Figure 5.
Monthly mean number of wet days for El Dorado Airport (Bogotá) Station for 1972–2015 filtered by the ONI

less reliable. Therefore, we attempt, instead, to use GLM techniques to construct the relevant probability density functions. We do this by specifying the model directly with the time of year and the IRI data for ENSO forecast probabilities as independent variables. Nevertheless, although we have daily rainfall data between 1972 and 2015, we are not able to use all the data to train the linear models, because the ENSO forecast probabilities developed by the IRI have

only been public since 2005. As a result, model training is restricted to information from 2005 to 2015.

3.1 Estimating precipitation frequency

Table 1 shows the VGLM regression results for Model 2, Model 3 and Model 4. They share some general trends. The negativity of all significant parameters for p_i^{01}, the dry-to-wet daily probability estimated for month j–points to, in general, the tendency that rain is unlikely to fall tomorrow if it did not fall today. However, that expectation mainly holds for December and January only. In contrast, the positivity of all significant parameters in the regression results for p_i^{11}, the wet-to-wet daily probability estimated for month j–says that, if it rains today, it is likely to rain tomorrow, and this holds for most of the year.

In Model 3, the coefficient of the El Niño forecast probability is significant and negative for p_i^{01} at 1% and for p_i^{11} at 10%. In Model 4, the difference between the forecast probabilities is significant and negative for both p_i^{01} and p_i^{11} at the 1% level. The Akaike information criterion (AIC), which tests the relative quality of statistical models (Akaike, 1974), performs better for the models that include the ENSO forecast probabilities.

	p_i^{01}			p_i^{11}		
Models	Model 2	Model 3	Model 4	Model 2	Model 3	Model 4
January	−1.24***	−1.08***	−1.26***	0.04	0.10	−0.02
	(0.16)	(0.16)	(0.16)	(0.20)	(0.20)	(0.20)
February	−0.84***	−0.73***	−0.91***	0.60***	0.65***	0.53***
	(0.17)	(0.17)	(0.17)	(0.18)	(0.18)	(0.18)
March	−0.36**	−0.25	−0.39**	0.80***	0.83***	0.74***
	(0.16)	(0.17)	(0.17)	(0.16)	(0.16)	(0.16)
April	0.33	0.44**	0.34	1.33***	1.38***	1.33***
	(0.21)	(0.21)	(0.21)	(0.16)	(0.16)	(0.16)
May	0.28	0.44**	0.34*	1.12***	1.16***	1.13***
	(0.20)	(0.20)	(0.20)	(0.15)	(0.15)	(0.15)
June	−0.13	0.01	−0.09	0.89***	0.96***	0.93***
	(0.18)	(0.18)	(0.18)	(0.15)	(0.16)	(0.15)
July	−0.03	0.20	0.08	0.66***	0.76***	0.73***
	(0.17)	(0.17)	(0.17)	(0.15)	(0.16)	(0.15)
August	0.14	0.33*	0.19	0.48***	0.56***	0.52***
	(0.17)	(0.18)	(0.17)	(0.14)	(0.15)	(0.15)
September	−0.40***	−0.18	−0.32**	0.35**	0.42**	0.36**
	(0.16)	(0.17)	(0.16)	(0.16)	(0.16)	(0.16)
October	0.26	0.48**	0.34*	0.87***	0.96***	0.89***
	(0.19)	(0.20)	(0.19)	(0.15)	(0.15)	(0.15)
November	0.02	−0.25	0.11	0.92***	1.00***	0.93***
	(0.18)	(0.15)	(0.19)	(0.15)	(0.16)	(0.15)
December	−0.77***	−1.52***	−0.73***	0.35**	0.42**	0.32**
	(0.16)	(0.20)	(0.16)	(0.16)	(0.17)	(0.16)
$p_j^{\text{Niño}}$		−0.54***			−0.25*	
		(0.14)			(0.13)	
$p_j^{\text{Niño}} - p_j^{\text{Niña}}$			−0.33***			−0.30***
			(0.08)			(0.08)
Observations	1741	1741	1741	2,275	2,275	2,275
AIC	2289.2	2276.2	2276.1	2829.0	2827.3	2815.4
BIC	2354.7	2347.2	2347.1	2897.7	2901.8	2889.9

Note(s): Standard errors are in parentheses. ***$p < 0.01$, **$p < 0.05$, *$p < 0.10$

Table 1.
VGLM regression results for the rainfall frequency process

A different approach to model adequacy is to check the root mean square error between a simulation and the historical series. Table 2 shows the RMSE for each month and for the entire analysis period (2005–2015) for 10,000 Monte Carlo paths with Model 2, Model 3 and Model 4. Model 3, which includes the probability of El Niño, has lower RMSEs than Model 2 in seven out of twelve months, but the total RMSE of Model 3 is inferior by a 1.50% margin. If we substitute the difference in the probabilities of El Niño and La Niña for the probability of El Niño, the RMSE is lower, compared to Model 2, in eight out of twelve months, by 2.86%. In summary, including the probability forecast for El Niño and La Niña improves the accuracy of the precipitation frequency model.

3.2 Estimating the daily precipitation amount

Table 3 shows the gamma-VGLM regression results for Model 2, Model 3 and Model 4. They share some common trends in terms of monthly significance. Nevertheless, the level of significance associated with $p_j^{\text{Niño}}$ is weaker than the corresponding difference of probabilities. Unlike the results for the expected rainfall μ_j, the weak to non-existent significance of the coefficients for the forecast probabilities suggests that the shape of the distribution is not very sensitive to the onset of ENSO-related phenomena.

Table 4 shows the RMSE for each month and for the entire analysis period (2005–2015) for the 10,000 paths of the Monte Carlo simulation for Model 2, Model 3 and Model 4. Model 3, which includes the probability of El Niño, has lower RMSEs than Model 2 for ten out of twelve months, excluding the rainiest months in Colombia, April and October (Figure 2). If we substitute the difference between the forecast probabilities of El Niño and La Niña for the probability of El Niño, the RMSE is between Model 2 and Model 3. In summary, the inclusion of El Niño and La Niña decreases the RMSE of the modeled daily precipitation amount.

3.3 Estimating the monthly precipitation amount and rainfall derivative prices

To simulate the monthly precipitation amount (I), we run 1,000 iterations of Model 3 and Model 4 using our Monte Carlo simulation. Table 5 shows the RMSE for each month over the entire period (2005–2015). The performances of Model 3 and Model 4 are similar. Therefore, including the forecast probabilities associated with El Niño and La Niña increases the accuracy of the precipitation frequency models.

Based on the historical forecast probabilities issued by the IRI for the occurrence of El Niño and La Niña, the frequency and daily amount models allow the monthly precipitation to be simulated in a way that minimizes RMSE. From this, and appropriate application of the

	Model 2	Model 3	Model 4
January	2.1932	2.1284	2.1374
February	2.2953	2.2545	2.2361
March	2.3163	2.2389	2.2123
April	2.0590	2.0894	2.0919
May	2.2949	2.2733	2.2245
June	2.1643	2.2035	2.1820
July	2.2382	2.2765	2.2817
August	1.9328	1.9574	1.9564
September	2.2505	2.1135	2.0804
October	2.1006	1.9935	1.9421
November	2.1727	2.0754	1.9994
December	2.3301	2.3469	2.2573
Total	2.1986	2.1657	2.1365

Table 2.
Root-mean-square error (RMSE) of the precipitation frequency simulation using Model 2, Model 3 and Model 4

Table 3.
VGLM regression results for the daily precipitation amount

Models	$\log(\mu_j)$ Model 2	$\log(\mu_j)$ Model 3	$\log(\mu_j)$ Model 4	$\log(\kappa_j)$ Model 2	$\log(\kappa_j)$ Model 3	$\log(\kappa_j)$ Model 4
January	−1.853***	−1.761***	−1.949***	−0.485***	−0.413***	−0.473***
	(0.125)	(0.123)	(0.124)	(0.117)	(0.119)	(0.117)
February	−1.706***	−1.625***	−1.811***	−0.472***	−0.428***	−0.467***
	(0.107)	(0.106)	(0.106)	(0.100)	(0.102)	(0.101)
March	−1.466***	−1.391***	−1.544***	−0.480***	−0.456***	−0.484***
	(0.092)	(0.092)	(0.092)	(0.086)	(0.087)	(0.087)
April	−1.348***	−1.231***	−1.356***	−0.527***	−0.516***	−0.529***
	(0.084)	(0.085)	(0.084)	(0.077)	(0.078)	(0.077)
May	−1.464***	−1.362***	−1.465**	−0.514***	−0.482***	−0.501***
	(0.084)	(0.084)	(0.083)	(0.077)	(0.078)	(0.077)
June	−1.955***	−1.814***	−1.938***	−0.531***	−0.463***	−0.498***
	(0.091)	(0.092)	(0.090)	(0.083)	(0.086)	(0.083)
July	−2.238***	−2.051***	−0.443***	−0.506***	−0.435***	−0.443***
	(0.090)	(0.093)	(0.084)	(0.083)	(0.088)	(0.084)
August	−2.216***	−2.040***	−2.195***	−0.385**	−0.327***	−0.360***
	(0.085)	(0.088)	(0.085)	(0.085)	(0.088)	(0.085)
September	−1.955***	−1.797***	−1.959***	−0.490***	−0.455***	−0.486***
	(0.101)	(0.102)	(0.101)	(0.094)	(0.096)	(0.094)
October	−1.376***	−1.153***	−1.362***	−0.530***	−0.522***	−0.540***
	(0.087)	(0.091)	(0.087)	(0.079)	(0.083)	(0.079)
November	−1.399***	−1.205***	−1.415***	−0.435***	−0.408***	−0.419***
	(0.085)	(0.089)	(0.085)	(0.082)	(0.085)	(0.082)
December	−1.575***	−1.420***	−1.628***	−0.451***	−0.390***	−0.428***
	(0.100)	(0.101)	(0.099)	(0.095)	(0.098)	(0.096)
$p_j^{\text{Niño}}$		−0.628***			−0.081	
		(0.079)			(0.074)	
$p_j^{\text{Niño}} - p_j^{\text{Niña}}$			−0.312***			−0.0742*
			(0.045)			(0.042)
Log-likelihood	1795.46	1825.38	1819.64	1795.46	1825.38	1819.64
AIC	−3542.92	−3587.33	−3598.76	−3542.92	−3587.33	−3598.76
BIC	−3405.40	−3438.36	−3449.79	−3405.40	−3438.36	−3449.79

Note(s): Standard errors are in parentheses. ***$p < 0.01$, **$p < 0.05$, *$p < 0.10$

Esscher transform, it is then possible to price simple European weather derivatives. The pricing framework developed in section 2.2 for monthly precipitation amount as underlying weather index produces the results of this procedure for two January derivatives, a call option (c_j) and a put option (p_j). Figure 6 illustrates the price behavior predicted by Model 3, and Figure 7 shows the corresponding results for Model 4. Each derivative is shown for three different values of the MPR parameter. The risk-free interest rate is 2.325%. All prices are estimated for a strike price (K) equal to 1 inch and an (arbitrary) tick of $1.

As found in the results of the VGLM regression for the rainfall frequency process and the daily precipitation amount, the increase in forecast probability of El Niño generates a decrease in the expected monthly rainfall amount. Therefore, an increase in the forecast probability of El Niño produces a substantial decrease in the call option price while increasing the put option price, as shown in Figure 6. For this particular case, when the probability of El Niño reaches 1, the reduction in the call option's price is approximately 91%, and the increase in the put option's price is approximately 634%, compared with a probability of 0.

Model 4 is based on the belief that, instead of specifying a model with separate forecast probabilities for the occurrence of El Niño or La Niña, it is better to assume that their difference better stronger characterizes the effects of ENSO on the conditional probability of a rainy day. This is the assumption that the difference Δ ($\Delta = p_j^{\text{Niño}} - p_j^{\text{Niña}}$) is a proxy for the

Models	Model 2	Model 3	Model 4
January	0.0791	0.0595	0.0700
February	0.0848	0.0624	0.0719
March	0.0839	0.0661	0.0748
April	0.0862	0.0944	0.1025
May	0.0923	0.0884	0.0948
June	0.0681	0.0590	0.0634
July	0.0554	0.0464	0.0451
August	0.0356	0.0246	0.0306
September	0.0755	0.0695	0.0750
October	0.0797	0.0966	0.0953
November	0.0927	0.0890	0.0885
December	0.1040	0.0797	0.0893
Total	0.0800	0.0726	0.0778

Table 4. Root-mean-square error (RMSE) of the daily precipitation amount simulated using Model 2, Model 3 and Model 4

Models	Model 1	Model 2	Model 3	Model 4
January	1.1672	1.0903	0.9736	1.0120
February	1.3553	1.3005	1.1549	1.2001
March	1.6094	1.5613	1.4866	1.4909
April	1.7763	1.6367	1.6945	1.7066
May	1.7789	1.6377	1.6274	1.6189
June	1.4634	1.2866	1.2268	1.2408
July	1.4641	1.0980	1.0639	1.0433
August	1.3550	0.9942	0.9123	0.9457
September	1.3623	1.2056	1.1147	1.1387
October	1.7190	1.5365	1.5840	1.5486
November	1.6835	1.6225	1.5275	1.4729
December	1.4260	1.3705	1.2596	1.2513
Total	1.5250	1.3800	1.3277	1.3283

Table 5. Root-mean-square error (RMSE) of the monthly precipitation amount simulated using Model 1, Model 2, Model 3 and Model 4

degree of certainty the forecaster has about the onset of a possible ENSO cycle. An increase in Δ generates a decrease in the probability of the monthly amount of rainfall, which affects the call and put option prices. A decrease in Δ increases the probability of a monthly amount of rainfall, widening the gap between the prices of call and put options. When Δ runs from -1 to 1, the call option price contracts by 92% and the put option price grows by 1,385%.

As seen in Figures 6 and 7, the rainfall indexes simulated using Model 3 and Model 4 produce similar behavior, with Model 4 producing a slightly better price discrimination for the different MPR sensitivities considered.

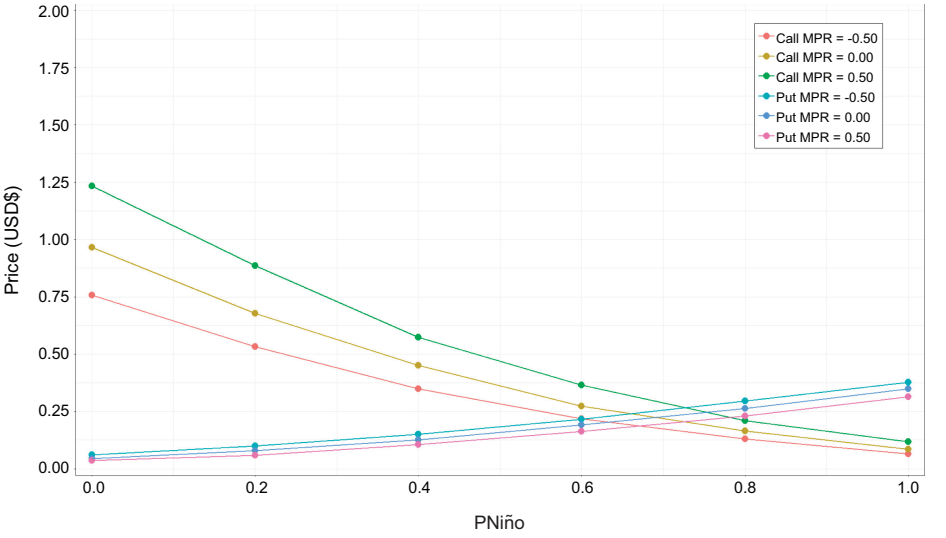

Figure 6.
Rainfall derivative prices using the probability of El Niño—January: El Dorado (Bogotá) Airport Station

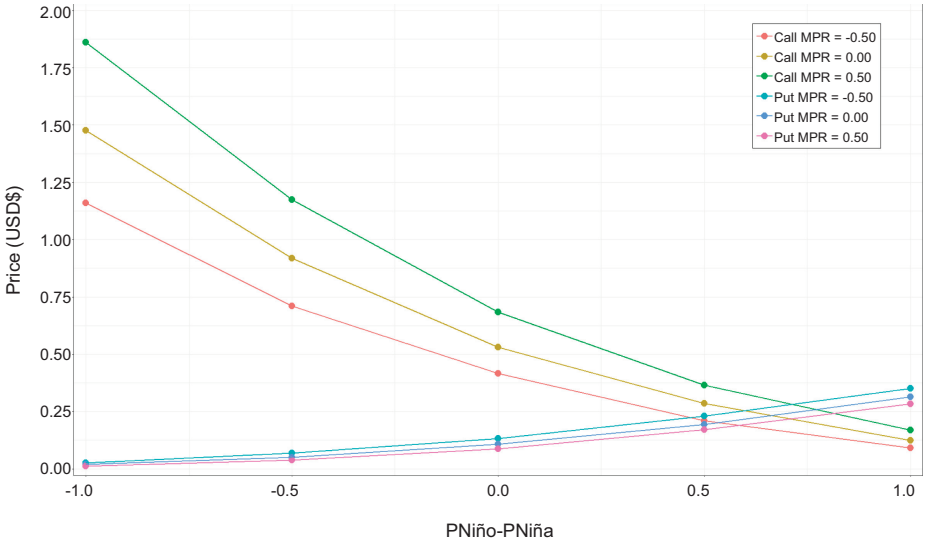

Figure 7.
Rainfall derivative prices using the difference between the probabilities of El Niño and La Niña—January: El Dorado (Bogotá) Airport Station

4. Conclusions

In this paper, we develop a complete framework suitable for valuing rainfall derivatives in the equatorial Pacific. The presence of rainfall extremes associated with the ENSO phenomenon makes this task both more challenging and necessary as an instrument for hedging weather risks in those latitudes. To achieve this goal, we start by following the general approach of Cabrera *et al.* (2013), who use the Esscher transform to build an appropriate risk-neutral martingale with which to compute derivative prices. This procedure introduces the market price of risk (MPR) to value rainfall derivatives under risk-neutral probabilities. Their approach follows strictly statistical methods to derive the necessary values for the daily conditional probability of rainfall and obtain the best fit for the probability distribution density given a monthly amount of rainfall.

Due to the considerable differences in weather patterns and challenged by the inadequacy of the data provided by the Oceanic Niño Index (ONI), we address the need for a different method of simulating the probability distribution of the rainfall index. In this paper, we construct a frame based on GLM estimation of the conditional probabilities for daily rainfall and for the estimation of the parameters of a gamma distribution fitted to the monthly rainfall distribution function. The precipitation frequency is then modeled using a two-state Markov process. The results of this modeling scheme were compared with other schemes without ENSO effects that were trained on the same data set to confirm that it leads to more accurate models of the conditions of the equatorial Pacific. The independent factors in the regression are the forecast probabilities issued by the IRI for the occurrence of El Niño and La Niña. This is new in the sense that these independent variables are related to physical, climatic measurements. The regression model also includes the month as an independent variable.

References

Aceituno, P. (1988), "On the functioning of the southern oscillation in the south american sector. Part I: surface climate", *Monthly Weather Review*, Vol. 116 No. 3, pp. 505-524.

Akaike, H. (1974), "A new look at the statistical model identification", *IEEE Transactions on Automatic Control*, Vol. 19 No. 6, pp. 716-723.

Alexandridis, A.K. and Zapranis, A.D. (2013), *Weather Derivatives: Modeling and Pricing Weather-Related Risk*, Springer, New York.

Barnston, A.G., Tippett, M.K., L'Heureux, M.L., Li, S. and DeWitt, D.G. (2012), "Skill of real-time seasonal enso model predictions during 2002-11: is our capability increasing?", *Bulletin of the American Meteorological Society*, Vol. 93 No. 5, pp. 631-651.

Benth, F.E. and Benth, Š. (2013), "Modeling and pricing in financial markets for weather derivatives", *World Scientific*, Singapore, Vol. 17.

Brockett, P.L., Wang, M., Yang, C. and Zou, H. (2006), "Portfolio effects and valuation of weather derivatives", *Financial Review*, Vol. 41 No. 1, pp. 55-76.

Cabrera, B.L., Odening, M. and Ritter, M. (2013), "Pricing rainfall derivatives at the CME", Humboldt-Universität zu Berlin, Wirtschaftswissenschaftliche Fakultät.

Cao, M. and Wei, J. (2004), "Weather derivatives valuation and market price of weather risk", *Journal of Futures Markets: Futures, Options, and Other Derivative Products*, Vol. 24 No. 11, pp. 1065-1089.

Cao, M., Li, A. and Wei, J. (2004), "Precipitation modeling and contract valuation", *Journal of Alternative Investments*, Vol. 7 No. 2, pp. 93-99.

Carmona, R. and Diko, P. (2005), "Pricing precipitation based derivatives", *International Journal of Theoretical and Applied Finance*, Vol. 8 No. 07, pp. 959-988.

Carr, P., Geman, H. and Madan, D.B. (2001), "Pricing and hedging in incomplete markets", *Journal of Financial Economics*, Vol. 62 No. 1, pp. 131-167.

Climate Prediction Center - NOAA (2019a), "National weather service", Available at: https://origin.cpc.ncep.noaa.gov/products/analysis_monitoring/ensostuff/ONI_v5.php (accessed 6 June 2019).

Climate Prediction Center - NOAA (2019b), "Annual Composites - Sea surface temperature (SST) anomaly during 1997", available at: ftp://ftp.star.nesdis.noaa.gov/pub/sod/mecb/crw/data/5km/v3.1/nc/v1.0/annual/ct5km_baa-max_v3.1_1997.nc (accessed 8 May 2019).

Climate Prediction Center - NOAA (2019c), "Annual Composites - Sea surface temperature (SST) anomaly during 1988", available at: ftp://ftp.star.nesdis.noaa.gov/pub/sod/mecb/crw/data/5km/v3.1/nc/v1.0/annual/ct5km_baa-max_v3.1_1988.nc (accessed 8 May 2019).

CME (2005), "An introduction to cme weather products", available at: https://www.cmegroup.com/trading/weather/ (accessed 3 May 2019).

Coles, S., Pericchi, L.R. and Sisson, S. (2003), "A fully probabilistic approach to extreme rainfall modeling", *Journal of Hydrology*, Vol. 273 Nos 1-4, pp. 35-50.

Dischel, B. (2000), "Seeding a rain market", *Environmental Finance*, September, pp. 2-4.

Esscher, F. (1932), "On the probability function in the collective theory of risk", *Skand. Aktuarie Tidskr*, Vol. 15, pp. 175-195.

Foufoula-Georgiou, E. and Lettenmaier, D.P. (1987), "A Markov renewal model for rainfall occurrences", *Water Resources Research*, Vol. 23 No. 5, pp. 875-884.

Gerber, H.U. and Shiu, E.S. (1994), "Option pricing by esscher transforms", *Transactions of society of actuaries*, Vol. 46, pp. 99-192.

Gerber, H.U. and Shiu, E.S. (1996), "Actuarial bridges to dynamic hedging and option pricing", *Insurance: Mathematics and Economics*, Vol. 18 No. 3, pp. 183-218.

Goncu, A. (2011), "Modeling and pricing precipitation-based weather derivatives", *Financial Mathematical Application*, Vol. 1 No. 1, pp. 9-18.

Grimm, A.M. and Tedeschi, R.G. (2009), "Enso and extreme rainfall events in south America", *Journal of Climate*, Vol. 22 No. 7, pp. 1589-1609.

Härdle, W.K. and Osipenko, M. (2011), *Pricing Chinese Rain: A Multisite Multi-Period Equilibrium Pricing Model for Rainfall Derivatives*, SFB 649 Discussion Paper 055, Humboldt-Universität zu, Berlin.

Instituto de Hidrología and Meteorologá y Estudios Ambientales (IDEAM) (2019), "Instituto de hidrologá, meteorologá y estudios ambientales", available at: http://www.ideam.gov.co/ (accessed 04 June 2019).

Jewson, S. and Brix, A. (2005), *Weather Derivative Valuation: The Meteorological, Statistical, Financial and Mathematical Foundations*, Cambridge University Press, Cambridge.

Lee, Y. and Oren, S.S. (2010), "A multi-period equilibrium pricing model of weather derivatives", *Energy Systems*, Vol. 1 No. 1, pp. 3-30.

Leobacher, G. and Ngare, P. (2011), "On modelling and pricing rainfall derivatives with seasonality", *Applied Mathematical Finance*, Vol. 18 No. 1, pp. 71-91.

Little, M.A., McSharry, P.E. and Taylor, J.W. (2009), "Generalized linear models for site-specific density forecasting of UK daily rainfall", *Monthly Weather Review*, Vol. 137 No. 3, pp. 1029-1045.

Martin, S.W., Barnett, B.J. and Coble, K.H. (2001), "Developing and pricing precipitation insurance", *Journal of Agricultural and Resource Economics*, Vol. 26, p. 261.

Mathai, A. (1982), "Storage capacity of a dam with gamma type inputs", *Annals of the Institute of Statistical Mathematics*, Vol. 34 No. 3, pp. 591-597.

Moreno, M. (2002), *Rain Risk. Research Paper*, Speedwell Weather Derivatives, London.

Moschopoulos, P.G. (1985), "The distribution of the sum of independent gamma random variables", *Annals of the Institute of Statistical Mathematics*, Vol. 37 No. 1, pp. 541-544.

Noven, R.C., Veraart, A.E. and Gandy, A. (2015), "A lévy-driven rainfall model with applications to futures pricing", *AStA Advances in Statistical Analysis*, Vol. 99 No. 4, pp. 403-432.

Odening, M., Mußhoff, O. and Xu, W. (2007), "Analysis of rainfall derivatives using daily precipitation models: opportunities and pitfalls", *Agricultural Finance Review*, Vol. 67 No. 1, pp. 135-156.

Prabahu, N. (1965), *Queues and Inventories: A Study of Their Basic Stochastic Processes*, John Wiley & Sons, New York.

Ropelewski, C.F. and Halpert, M.S. (1987), "Global and regional scale precipitation patterns associated with the el niño/southern oscillation", *Monthly Weather Review*, Vol. 115 No. 8, pp. 1606-1626.

Spicka, J. and Hnilica, J. (2013), "A methodical approach to design and valuation of weather derivatives in agriculture", *Advances in Meteorology*, Vol. 2013, Article 146036, p. 2013.

Suhaila, J. and Jemain, A.A. (2007), "Fitting daily rainfall amount in peninsular Malaysia using several types of exponential distributions", *Journal of Applied Sciences Research*, Vol. 3 No. 10, pp. 1027-1036.

Turvey, C.G. (2001), "Weather derivatives for specific event risks in agriculture", *Applied Economic Perspectives and Policy*, Vol. 23 No. 2, pp. 333-351.

Wilks, D.S. (1989), "Rainfall intensity, the weibull distribution, and estimation of daily surface runoff", *Journal of Applied Meteorology*, Vol. 28 No. 1, pp. 52-58.

Wilks, D. (1998), "Multisite generalization of a daily stochastic precipitation generation model", *Journal of Hydrology*, Vol. 210 Nos 1-4, pp. 178-191.

Wilks, D.S. (2011), *Statistical Methods in the Atmospheric Sciences*, Academic Press, San Diego, Vol. 100.

WRMA, (2011), "The weather risk management association (wrma)", available at: https://wrma.org/ (accessed 03 September 2019).

Xu, W., Odening, M. and Mußhoff, O. (2008), "Indifference pricing of weather derivatives", *American Journal of Agricultural Economics*, Vol. 90 No. 4, pp. 979-993.

Yu, J.-Y., Kao, H.-Y., Lee, T. and Kim, S.T. (2011), "Subsurface ocean temperature indices for central-pacific and eastern-pacific types of el niño and la niña events", *Theoretical and Applied Climatology*, Vol. 103 Nos 3-4, pp. 337-344.

Appendix

Probability function of the rainfall index

The Esscher transform (Esscher, 1932):

$$f_Q(x;\pi) = \frac{\exp(\pi x) f_P(x)}{\int_{-\infty}^{\infty} \exp(\pi x) f(x)_P dx} \tag{A.1}$$

where π is the market price of the risk (MPR). The probability function of the rainfall index I during n wet days is:

$$f_P(I;\kappa,\theta) = \sum_{n=1}^{m} \frac{\theta^{-n\kappa} I^{n\kappa-1} \exp\left(\frac{-I}{\theta}\right)}{\Gamma(n\kappa)} g(n) \tag{A.2}$$

where m is the number of days in the month and $g(n)$ describes the probability of having n wet days. The Esscher transformation of the probability function of $I(n)$ given π (MPR) is defined as:

$$f_Q(I;\pi,\kappa,\theta) = \frac{\exp(\pi I)\sum_{n=1}^{m} \frac{\theta^{-n\kappa} I^{n\kappa-1} \exp\left(\frac{-I}{\theta}\right)}{\Gamma(n\kappa)} g(n)}{\int_0^{+\infty} \exp(\pi I)\sum_{n=1}^{m} \frac{\theta^{-n\kappa} I^{n\kappa-1} \exp\left(\frac{-I}{\theta}\right)}{\Gamma(n\kappa)} g(n) dI} \tag{A.3}$$

$$f_Q(I;\pi,\kappa,\theta) = \frac{\exp(\pi I)\sum_{n=1}^{m} \frac{\theta^{-n\kappa} I^{n\kappa-1} \exp\left(\frac{-I}{\theta}\right)}{\Gamma(n\kappa)} g(n)}{\int_0^{+\infty} \sum_{n=1}^{m} \frac{\theta^{-n\kappa}}{\Gamma(n\kappa)} I^{n\kappa-1} \exp\left(\pi I - \frac{I}{\theta}\right) g(n) dI} \tag{A.4}$$

$$f_Q(I;\pi,\kappa,\theta)=\frac{\exp(\pi I)\sum_{n=1}^{m}\frac{\theta^{-n\kappa}I^{n\kappa-1}\exp\left(\frac{-I}{\theta}\right)}{\Gamma(n\kappa)}g(n)}{\sum_{n=1}^{m}\frac{\theta^{-n\kappa}}{\Gamma(n\kappa)}g(n)\int_0^{+\infty}I^{n\kappa-1}\exp\left(I\frac{\pi\theta-1}{\theta}\right)dI} \tag{A.5}$$

$$f_Q(I;\pi,\kappa,\theta)=\frac{\exp(\pi I)\sum_{n=1}^{m}\frac{\theta^{-n\kappa}I^{n\kappa-1}\exp\left(\frac{-I}{\theta}\right)}{\Gamma(n\kappa)}g(n)}{\sum_{n=1}^{m}\frac{\theta^{-n\kappa}}{\Gamma(n\kappa)}g(n)\frac{\Gamma(n\kappa-1+1)}{\left(I\frac{\pi\theta-1}{\theta}\right)^{(n\kappa-1+1)}}} \tag{A.6}$$

$$f_Q(I;\pi,\kappa,\theta)=\frac{\exp(\pi I)\sum_{n=1}^{m}\frac{\theta^{-n\kappa}I^{n\kappa-1}\exp\left(\frac{-I}{\theta}\right)}{\Gamma(n\kappa)}g(n)}{\sum_{n=1}^{m}\frac{\theta^{n\kappa-n\kappa}}{\Gamma(n\kappa)}g(n)\frac{\Gamma(n\kappa)}{(I[\pi\theta-1])^{(n\kappa)}}} \tag{A.7}$$

$$f_Q(I;\pi,\kappa,\theta)=\frac{\exp(\pi I)\sum_{n=1}^{m}\frac{\theta^{-n\kappa}I^{n\kappa-1}\exp\left(\frac{-I}{\theta}\right)}{\Gamma(n\kappa)}g(n)}{\sum_{n=1}^{m}\frac{g(n)}{(I[\pi\theta-1])^{(n\kappa)}}} \tag{A.8}$$

Corresponding author
Sergio Cabrales can be contacted at: s-cabral@uniandes.edu.co